

MaAST: Map Attention with Semantic Transformers for Efficient Visual Navigation

Zachary Seymour[†] Kowshik Thopalli* Niluthpol Mithun[†] Han-Pang Chiu[†] Supun Samarasekera[†] Rakesh Kumar[†]

Abstract—Visual navigation for autonomous agents is a core task in the fields of computer vision and robotics. Learning-based methods, such as deep reinforcement learning, have the potential to outperform the classical solutions developed for this task; however, they come at a significantly increased computational load. Through this work, we design a novel approach that focuses on performing better or comparable to the existing learning-based solutions but under a clear time/computational budget. To this end, we propose a method to encode vital scene semantics such as traversable paths, unexplored areas, and observed scene objects—alongside raw visual streams such as RGB, depth, and semantic segmentation masks—into a semantically informed, top-down egocentric map representation. Further, to enable the effective use of this information, we introduce a novel 2-D map attention mechanism, based on the successful multi-layer Transformer networks. We conduct experiments on 3-D reconstructed indoor PointGoal visual navigation and demonstrate the effectiveness of our approach. We show that by using our novel attention schema and auxiliary rewards to better utilize scene semantics, we outperform multiple baselines trained with only raw inputs or implicit semantic information while operating with an 80% decrease in the agent’s experience.

I. INTRODUCTION

Humans employ semantic scene structures to reason about the world and pay particular attention to relevant semantic landmarks to develop navigation strategies [1], [2]. Therefore, humans can efficiently learn from past navigation experience to explore new environments, such as discovering common semantic scene entities that can be generalized to similar but previously unseen places. The ultimate goal of visual navigation for autonomous agents is to enable agents to resemble or even exceed these human capabilities. A traditional approach to this problem is to localize the agent in a map of the environment that is built beforehand or constructed using simultaneous localization and mapping (SLAM) algorithms [3]–[5]. Paths are then planned to convey the agent to target locations [6]–[8]. These geometry-based methods require extensive hand-engineering, and cannot be easily applied to new unexplored environments.

Recently, learning-based methods—with deep reinforcement learning (DRL) leading the way, are being developed to address this problem. DRL methods directly learn a mapping from observations to actions through trial-and-error interactions with its environment. They have demonstrated promising results on navigation tasks and showed superior performance

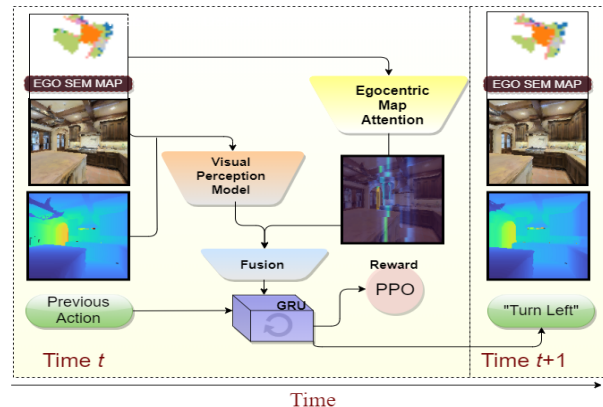


Fig. 1: We show an overall diagram of our proposed approach, MaAST. Given RGB and Depth inputs, as well as an accumulated top-down egocentric semantic map constructed by our system, the model uses features from both the visual perception model and our novel map attention module to predict its next action. In addition to the input images, we also visualize the learned semantic map attention, projected back onto the RGB observation.

compared to geometry-based methods [9]. However, current state-of-the-art DRL methods require training with massive amounts of observations to achieve satisfactory performance. They lack the semantic reasoning capabilities that humans possess to quickly learn from past experience and extrapolate to new environments. Hundreds of millions of interactions with the training environments, requiring enormous computational resources and distributed processing [10], are mandatory to converge to a reasonable policy for complicated scenarios.

In this paper, we take a step towards more efficient learning, as humans do: learning to achieve comparable (or better) visual navigation performance for autonomous agents with less available budget. The budget can be in terms of the number of data observations available to the agent, or the available computational resources (and, thus, time) available for training the model.

To achieve this objective, we propose to synergistically utilize the scene semantics along with a novel structured attention mechanism in a DRL model, which we call **Map Attention with Semantic Transformers**, or MaAST (Figure 1). We propose to first construct a memory structure in which we encode the semantic class of each object (or region) the agent perceives in the environment. We also introduce a novel formulation of the popular Transformer architecture [11], which we refer to as egocentric map Transformer, to encourage the agent to learn pertinent objects and regions based on their spatial relationship with the agent. This attention module

[†]SRI International; Email: firstname.lastname@sri.com

*Arizona State University; Email: kthopall@asu.edu

automatically focuses on relevant parts of the map memory structure so as to determine the next action to take.

Through this work, we make the following observations: i) a naïve data-driven approach of utilizing scene semantics provides no added benefit to using an egocentric occupancy map [12]; ii) on the other hand, we show that with our novel attention mechanism, we outperform multiple state-of-the-art approaches particularly in terms of path efficiency; and iii) through systematic ablation experiments, we establish empirically the superior efficacy of our proposed attention mechanism on semantic features. Our observations corroborate our hypothesis: just as humans do, autonomous agents should pay careful attention to semantic landmarks to obtain improved performance. Thus, the contributions of our proposed approach, MaAST, are as follows:

- 1) To the best of our knowledge, we present the first study on the effective use of perceived scene semantics and their spatial arrangement to train an agent end-to-end on the task of visual navigation in unseen environments.
- 2) We introduce a novel 2-D map attention mechanism, based on Transformers, for encouraging model to extract features from and to focus on the most relevant areas of structured, egocentric, top-down spatial information.
- 3) We demonstrate significant improvements in the policy’s performance metrics and sample efficiency when learned under restricted training budgets.

II. RELATED WORK

DRL for Navigation: There is a recent surge of interest in using learning-based methods and DRL for visual navigation, and consequently, a number of methods have been proposed [10], [12]–[19]. Due to the prohibitive costs associated with physically training agents with DRL, most of the methods instead train agents in a simulator with multi-threaded implementations. To this end, several simulators, predominantly supporting indoor navigation, have been proposed [9], [17], [20]–[24]. Similarly, several 3D datasets have been collected for indoor navigation. Many are synthetic [25]–[27], based on CAD models and hence lacking realism, while others [22], [28], [29] consist of 3D scans of real environments. Thus, many recent works in visual navigation (including our own) focus on these photo-realistic datasets [9], [30]–[32].

Exploration and Mapping in DRL: It has been shown that a key factor for success in navigation is exploration; *i.e.*, to increase an autonomous agent’s coverage of a given area with efficacy [33], [34]. While [33] uses heuristics and [34] depends on a human controller to build maps and explore, recent works [12], [19], [35], [36] propose solutions to this task of exploration via learning. Our work is most closely related to recent works [12], [19], [37], [38] that address the problem of task-agnostic exploration, using DRL to learn effective exploration policies that maximize the coverage of a given environment. However, a key drawback in the use of top-down occupancy map [12], [19] is a failure to encode the diverse semantic cues such as doors, different rooms, *etc.* that humans use to explore or navigate. While several recent works

have begun to show promise in leveraging a hierarchical DRL policy combined with an analytical planner, our focus remains on improving the efficiency of end-to-end DRL solutions by improving the intermediate scene representation. We propose a novel solution which uses segmentation masks of the current observation to accumulate top-down, egocentric semantic maps. However, we find the richness contained in these maps adds additional complexity for the policy network to properly make use of these features. Consequently, we also introduce a novel multi-layer Transformer architecture for processing such 2-D top-down structured information, allowing more relevant features to be extracted.

Semantic Feature Fusion: It has been shown in prior works that semantic cues leads to improved performance in learning-based navigation methods [31], [39] as would intuition confirm it to be. However, these methods use the semantically-segmented images as direct inputs to the model, which directly discards information about the 3D structure of the scene. By contrast, we propose to use those cues to build better occupancy maps and thus a better memory structure for our policy, as opposed to extending RL agents with specialized memory structures such as [40], [41].

III. APPROACH

Problem Setup: In this work, we consider the task of PointGoal navigation; *i.e.*, given a specified starting location and orientation, the agent is required to navigate to the desired target location in an unseen cluttered environment. However, our proposed method is general and can be easily extended to other navigation tasks, such as ObjectGoal and AreaGoal tasks. We refer our readers to [42] for a concise description of these tasks. We assume that our navigation agents are equipped with an RGB camera and a Depth sensor. We also assume the agent has a semantic sensor, capable of producing semantic segmentation of the current RGB camera observation - a class number $c \in \{1, \dots, N_c\}$ for each pixel in the RGB image. Note our goal is to show increased learning efficacy of the agent, given an improved understanding of the scene.

Our objective is to learn a policy π through reinforcement learning that makes effective use of all three sensory outputs (RGB camera, Depth sensor, and the semantic sensor) for navigation. To achieve this, we propose a novel method to first construct and maintain an egocentric semantic map of the environment using the Depth and semantic sensors. We construct an image of the map such that the agent is at the center, and the map is rotated such that the agent’s heading points upwards. Previous work has shown that providing autonomous agents a local map of its surroundings enables stronger reward signals to reinforce learning and encourages exploration of new environments [12]. Our intuition is that enhancing the map with a structured semantic representation of the objects and regions in a scene will allow the agent to make better decisions with regards to its goal, in addition to exploring unseen areas. We finally propose a novel structured attention mechanism to extract information from the map, such that the policy network learns to focus on most relevant regions in the map to predict its next action.

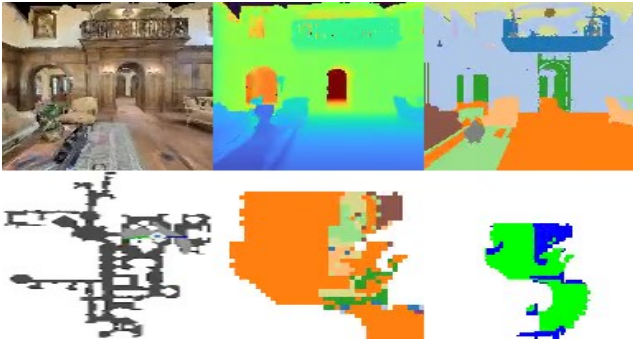


Fig. 2: An example of the observations available to the agents. Clockwise from top left: RGB; Depth, colored with Turbo [43]; semantic segmentation mask; occupancy map, where green denotes traversable space and blue obstacles; semantic map; a ground truth map of the traversed path (for visualization purposes only).

A. Egocentric Semantic Map Construction

For map construction, we primarily follow [12], in the setting where we assume no estimation error on the agent’s pose. Concisely, when an agent takes an action a_t at time step t , it receives a set of observations $O_{t+1} = (r_{t+1}, d_{t+1}, s_{t+1})$ representing the outputs from the RGB, Depth, and semantic sensors, respectively. The pixels in the depth image can be back-projected to a 3-D point cloud using the known camera intrinsic parameters. The extrinsic parameters can then be calculated from the agent’s current pose estimate to transform the point cloud from the camera’s reference frame to the world frame. The points are then projected down to form a 2-D map of the environment. Finally, the map is cropped to a fixed radius r around the agent such that the agent is at the center, of the image and is rotated such that the agent’s heading points upwards. In [12], three types of information are stored in the map. Any points above and below some height threshold are projected down and stored in the map as obstacles. The remaining points are stored as traversable space, and the rest of the map is treated as yet unexplored.

Information about traversable and non-traversable space is extremely useful to support path planning in autonomous agents; however, our intuition is that a large amount of this information, particularly for short-term action decisions, is encoded in depth image already, as evidenced by the strong performance of agents with only a depth sensor [30]. Although exploration and map-building allow the learned policy to better support back-tracking and movement to unexplored areas, we propose that discriminating different objects and free space is more useful for long-term decision making and reward prediction, particularly in large environments where an agent must traverse several rooms to achieve its goal.

Our approach is to enhance the information stored in the agent’s map of the environment with the semantic classes of perceived objects and components in the scene. That is, for each point categorized as an obstacle above, we instead store its semantic class (*e.g.*, the highest prediction class conditional probability of the pixel from semantic segmentation or value given from the semantic sensor) directly in the map. When there are instances of vertically overlapping objects (*e.g.*, lamp hanging over a table) or if the map resolution is low, some

points may be projected down into the same map location, resulting in a loss of information where one class overwrites others. As such, we instead treat each location in an $2r \times 2r$ map M as a binary vector $M_{ij} \in \{0, 1\}_c^N$ where, $k = 1$ if class k is present at that location and 0 otherwise. In this way, as the agent moves through the environment, it accumulates a map containing a bag-of-classes at each grid location. In addition to providing a richer source of information about the environment, this semantically enhanced map allows the same policy architecture to transit easily to other navigation tasks (*e.g.*, ObjectGoal) where the agent must identify semantics of its surroundings for successful goal achievement. Figure 2 shows an example, providing a visualization of the various observation modalities available to the agents.

B. Policy Architecture

An overall diagram of our policy architecture is shown in Figure 1. The network receives two sources of information, an RGB-D observation and a 2-D egocentric semantic map. Each of these is processed by a convolutional neural network (CNN) to produce visual and map feature vectors, respectively. We denote the RGB and Depth observations at time step t by (r_t, d_t) . The visual model, denoted f_{CNN} , transforms (r_t, d_t) to (r_t^{emb}, d_t^{emb}) by $f_{CNN}(r_t), f_{CNN}(d_t)$. In our experiments, we concatenate both RGB and Depth observations and transform them by f_{CNN} , obtaining the corresponding output as rd_t^{emb} ; for brevity and without loss of generality, we use r_t^{emb} to denote the same. While in prior work—where a policy is learned exclusively for exploration [12]—each f_{CNN} was implemented by a ResNet18 [44] CNN pretrained on Imagenet, we found the simpler, 3-layer CNN described in [9] to give better performance for navigation-oriented tasks.

We represent by f_{MAP} the network that transforms the egocentric semantic map at time step t , M_t (Section III-A). We consider two formulations of f_{MAP} . In the first case, f_{MAP} uses the same architecture as f_{CNN} : a 3-layer CNN. This mirrors the method used in [12], where the visual and map information are processed by two versions of the same network with different weights. However, because the information stored in our semantic map is much richer than that in the occupancy map, we find that the same CNN architecture is unable to adequately extract meaningful representations from it. Drawing inspiration from prior work in neural mapping and memory [40], we instead design a network for processing the map input by treating it like a memory unit. Unlike in [40], we would like to explicitly preserve the geometry and layout of the scene. We do not need to learn a specialized method to “write” to the memory. We only need to “read” (or extract feature) from it. To this end, we utilize a form of Transformer architecture [11], [45], adapted to use both a two-dimensional self-attention mechanism [46] and to learn specialized positional embeddings to better take advantage of the structured nature of the map input. It allows the network to better learn an representation of semantic classes present in the scene and to extract information about the relevant regions of the map. We next present our map attention mechanism, which is designed for this problem.

C. Egocentric Map Transformer

Our map attention mechanism is chiefly inspired by the use of the Transformers in natural language processing, which are deep neural networks consisting of multiple layers of multi-headed self-attention. In the case of natural language (*cf.* [11], [45]), the self-attention is generally computed using feature representations of each subword in a sentence, computed as the sum of two learned embeddings: a token embedding, which is specific to each subword, and a positional embedding, indicating the position of the token in a sentence. This composition allows the subword representation to vary depending on its location in the sentence.

Prior works using spatial or image-based self-attention have primarily operated on images [46] (where there is no direct analogue for the positional embedding) or on a sequence of image region features (in which case position encodings are drawn from alignment with corresponding words [47] or bounding box [48]). However, because the input to f_{MAP} consists of an $2r \times 2r \times N_c$ map centered on the agent, each map cell has important structural information. It is important to encode information about a cell based on its current relationship to the agent. Namely, for a map of radius r , we propose to construct a $2r \times 2r$ matrix of position indices \mathcal{P} using by a Gaussian kernel, centered on the agent, with a scale factor of $\frac{r}{2}$. As more of the mass of the Gaussian kernel is concentrated around the center, this has the benefit of giving fine-grained positional representations to map cells nearer the agent than those farther away (Figure 3).

Given such a kernel matrix, we construct \mathcal{P} by assigning each unique value in the kernel a unique consecutive integer, which are then used to index the learned positional embeddings. Thus, the sum of these embeddings and the bag-of-embeddings for the semantic classes at each cell are used as the input to the multi-layer Transformer.

We adapt each layer of the Transformer to utilize 1×1 convolutions to preserve the spatial dimensions of the map before pooling across both spatial dimensions and the final output. We denote this final transformed feature representation $f_{\text{MAP}}(M_t)$ by M_t^{emb} , with both $r_t^{\text{emb}}, M_t^{\text{emb}} \in \mathbb{R}^{N_h}$ and N_h is the hidden dimension of the policy network. The pooled outputs of f_{CNN} and f_{MAP} are finally concatenated, and fused by a fully-connected layer. The output along with the agent’s previous action is fed into a one-layer gated recurrent unit (GRU) [49], that enables the agent to maintain coherent action sequences across several time steps (the actor) followed by a linear layer (the critic) to predict the next action.

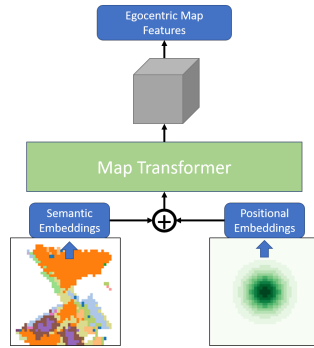


Fig. 3: An overview of proposed map Transformer module. The input semantic map (color-coded by class) is on the left and, the encoded positional indices (with colors becoming darker closer to the agent) is on the right.

TABLE I: Results of our proposed method, compared against several alternatives, evaluated for visual navigation on the Matterport3D validation set. We report both success weighted by path length (SPL) and episode success rate. †: uses our egocentric map Transformer.

Method	Map	Rewards		SPL (%)	Succ(%)
		Goal	Exploration		
RGB-D [9]	RL (PPO)	✓		34	51
RGB-D [9]	SLAM			42	-
RGBD+OCC [12]	RL (PPO)	Occupancy	✓	43	52
MaAST	RL (PPO)	Semantic†	✓	47	54

D. Rewards and Optimization

The network is trained end-to-end using reinforcement learning, particularly proximal policy optimization (PPO) [50], following [9]. All policies trained in this manner receive a reward R_t at time step t for moving closer to the goal equal to the change in distance to the goal plus a large reward s if the goal is reached and a small time penalty λ . For agents with access to a map of the environment, we also add an auxiliary reward equal to the percentage of map tiles that have been revealed, to encourage both exploration and better use of the map features. Our trained policies also include a small penalty for collisions with environment, equal to 0.01 λ .

IV. EVALUATION

Simulator and Dataset: We use Habitat simulator [9], which supports different datasets such as Matterport3D [28], Gibson [22], *etc.* We focus our experiments on Matterport3D [28], which consists of 3D reconstructions of 90 houses with a total of 2056 rooms, as it exhibits the greatest episodic complexity compared to the others. We use standard splits following [9]. It is to be noted that there is no overlap of scenes in the Matterport3D splits. We refer to [9] for more details.

Evaluation Metrics: An episode is registered as a success if (i) the agent has taken fewer than 500 steps, (ii) the distance between the agent and goal is less than 0.2m, and (iii) the agent takes STOP action to indicate that it has reached goal. The third condition eliminates a situation when the agent randomly stumbles upon the target and receives reward. We also report success weighted by path length (SPL) [42]. SPL is a measure of the efficacy of the policy’s path taken to the goal compared against the ground truth shortest path.

Implementation Details: Following [42], we use the same experimental setup as [9] for PointGoal navigation. We implemented the networks using PyTorch [51] and the habitat-sim and habitat-api modules [9]. For training, we use rollout size of 256, hidden dimension of 512, and learning rate of 10^{-4} . For our egocentric map Transformer, we adapt the implementation [52] as described in Section III-C. We use a 2-layer BERT model with 4 attention heads each and embeddings of size 128 for both positional and semantic embeddings. As in [9], we work with a case where our agents are equipped with an idealized GPS sensor and compass. Following the use of ground truth scene information (such as ground truth depth) in prior works [9], [10], [12], [53], we utilize the known depth and label of each pixel from the simulation environment to enable a fair comparison.¹

¹However, we experiment below leveraging MaAST with online predicted semantics, as well.

A. Quantitative Results

1) *Compared Methods*: We compare MaAST with several baselines in Table I on the MatterPort3D [28] validation set.

RL (PPO): The agents are trained end-to-end using DRL, namely PPO, with reward mechanism in Section III-D. We study the performance of RL-based agents with different input sensor modalities: RGB-D, with only RGB and Depth sensors as inputs; RGBD+OCC, the approach proposed in [12] (*i.e.*, along with RGB-D input, the method also uses a egocentric occupancy map), trained with both goal and exploration rewards. In prior work [12], the policy architecture was trained exclusively for exploration; however, in our case, it is trained by PPO end-to-end for PointGoal navigation.

While algorithms other than vanilla PPO have been recently applied in the visual navigation space to enable distributed training with large amounts of experience [10], a direct comparison with these methods is beyond the scope of this paper as i) DD-PPO is a DRL algorithm more than a specific visual navigation solution, and ii) we can easily train MaAST with any proven RL algorithm to achieve performance boosts from more efficient, large-scale training. Further, while recent works have shown the success of using hierarchical DRL policies paired with analytical planners such as A* in exploration and navigation [19], [37], we restrict our focus on learning and improving end-to-end RL policies with simpler modules. Our proposed approach (incorporating important semantic scene information into the map) can be incorporated with [19] as we did with [12]. We leave it as a future work.

As our main objective is to show MaAST’s effectiveness under budget constrained situations, we evaluate all the methods under a fixed training budget of 14 million steps of experience, as this was the point at which a Depth agent has been shown to exceed performance of SLAM [9].

2) *Analysis of Results*: In Table I, we demonstrate that the proposed approach (MaAST) significantly outperforms other methods and baselines, under a much reduced computational load. Agents equipped with no visual sensors (*i.e.*, blind) are expected to show poor performance. Surprisingly, a blind agent [9] trained by PPO is already able to achieve a modest success (35%) with 75 million steps of training experience. However, agents equipped with visual sensors show large performance improvement with reduced experience.

Among agents equipped with visual sensors, MaAST shows significant improvement over other agents. The improvement is +13% absolute (+38% relative) in SPL as compared to RGB-D alone and +4% absolute (+9% relative) as compared to RGBD+OCC. In terms of success rate, the performance increase is comparatively less (+6% relative over RGB-D and +4% relative over RGBD+OCC). This shows that even though most of the methods succeed at nearly the same rate, MaAST’s policy demonstrates superior efficacy in producing shorter paths to the target, due to our attention mechanism’s ability to focus on more relevant parts of the map, such as potential collisions or new areas to explore. With respect to the statistical significance of our results, we evaluated the performance of MaAST averaged over 5 random seeds and obtained SPL of 47.5 ± 0.7 , making the performance

TABLE II: Ablation study of the proposed MaAST on Matterport3D. All models are evaluated after training for 14 million steps of experience using RL (PPO). †: uses our egocentric map Transformer.

	Method	Map	SPL (%)	Succ(%)
MaAST w/o (EXP, SEM, ATT)	RGB-D		34	51
MaAST w/o (SEM, ATT)	RGBD+EXP		38	53
MaAST w/o ATT	RGBD+SEM	Semantic	41	49
MaAST w/o SEM, + OCC	RGBD+OCC+ATT	Occupancy†	44	52
MaAST	RGBD+SEM+ATT	Semantic†	47	54

gain over other compared methods roughly an order of magnitude greater than the standard deviation of MaAST’s performance. Furthermore, we note that MaAST is able to achieve significant improvements over SLAM in only 14 million training steps, which could not be achieved by RGB-D alone in prior work, even with five times more experience [9].

B. Ablation Study

To investigate the impact of different components of our proposed MaAST, we perform an ablation study comparing several baselines in Table II. All the methods in Table II are trained with both goal and exploration rewards except RGB-D which is trained with only goal rewards.

Exploration Rewards. We can compare RGB-D and RGBD+EXP baselines in Table II to evaluate the impact of the addition of exploration reward. RGB-D agent performs reasonably well with a 51% success rate. However, as seen in the SPL of RGB-D (34%), the agent takes much longer paths as compared to the ground-truth shortest distance, thus rendering this policy inefficient in terms of path length. We hypothesize this drop is due to the agent being not able to make efficient use of the implicit semantic cues in the scene.

To encourage the agent to move more efficiently, we follow a similar procedure as above to train a policy that utilizes RGB-D along with additional exploration reward: RGBD+EXP. However, the agent has no explicit access to the progressively growing, egocentric occupancy map. The method achieves a 4% increase in SPL (38%); thus, the addition of exploration reward not only helps the agent reach its goals more often but also takes more efficient paths to do so.

Egocentric Semantic Map. It is evident from Table II that our use of egocentric semantic map leads to an overall improvement in performance. To analyze the impact, we can compare several variants of MaAST (*i.e.*, RGBD+OCC+ATT vs. MaAST, and RGBD+EXP vs. RGBD+SEM). We observe that MaAST achieves (+3% absolute, 7% relative) improvement in SPL and (+2% absolute, 4% relative) improvement in success rate using egocentric semantic map compared to RGBD+OCC+ATT (which uses egocentric occupancy map). However, comparing RGBD+SEM to RGB-D, we find that use of semantic map helps RGBD+SEM to achieve +3% improvement in SPL, but there is a drop in performance in terms of success rate (−2%). We suspect this is because the information encoded in the egocentric semantic map is rich, however, the agent is unable to adequately decode and focus on relevant parts of the map (which inspires our use of the Transformer-based map attention mechanism).

Real vs. Predicted Semantics. To better measure the robustness of our method to sensor noise, we conducted an experiment utilizing predicted semantic segmentation,

following the map construction method of [38]; *i.e.*, segment the RGB observation with Mask R-CNN trained on MSCOCO and project those classes using `Depth`. This yields a sparser map now with 80 semantic classes rather than 40 from Matterport3D, and now only filled with confident predictions from the semantic segmentation model rather than dense labels for each pixel. Due to computational constraints, we train this model for 7.7 million steps of experience, at which point it achieves 34.8% SPL outperforming our RGB-D results with about half as much experience. This demonstrates the robustness of MaAST to even noisy semantic observations and its ability to adapt them to efficient navigation.

Egocentric Map Transformer. Our novel attention (ATT) mechanism based on multi-layer egocentric map Transformer leads to significant improvement in performance (Table II). We observe that MaAST achieves large performance improvement in SPL, compared to RGBD+EXP (+9%) and RGBD+SEM (+6%), due to the effective use of semantic cues. However, despite having access to the semantic map, RGBD+SEM fails to achieve consistent performance improvement over RGBD+EXP. This phenomenon supports our hypothesis that egocentric map transformer helps agents attend to most relevant regions of the map for efficient navigation.

We also use the proposed egocentric map Transformer (Section III-C) with the occupancy map (RGBD+OCC+ATT). However, this does not result in a noticeable change in performance. We believe this is because of the information encoded in the egocentric occupancy map is significantly less rich and less diverse compared to the semantic map. Rather than encoding each map cell to about 40 semantic classes in the egocentric semantic map, each occupancy map cell encodes either *unexplored*, *traversable*, and *non-traversable*.

C. Qualitative Results

In Figure 4, we provide some visualizations of the paths toward the goal followed by the various methods in three different episodes from the Matterport3D validation set. In the top row (Figures 4a–4c), we compare MaAST with RGBD+EXP, and RGBD+SEM. In the bottom row (Figures 4d–4f), we compare against our two baselines from prior work, RGB-D and RGBD+OCC. All methods have their path colored with a gradient to capture the number of steps taken by the agent, all scaled between 0 and 500 steps. For example, in Figure 4e, RGB-D agent moves quickly towards the goal at first; however, it becomes stuck behind a chair. When it moves away, its path is much more darkly colored, to indicate the amount of time taken to recover from the obstacle.

In the first episode (Figures 4a and 4d), all the agents reach the goal, but the RGB-D and RGBD+EXP take very long paths to do so. It is clear that RGBD+EXP tends to very aggressively follow the available traversable space, which leads to inefficient paths (Figure 4b) or missing the goal entirely (Figure 4c). Figures 4b–4e all help to demonstrate the efficiency gains of the MaAST attention mechanism. Even in cases where several of the methods follow similar paths to the goal, MaAST is more quickly able to find obscured free space (such as around the obstacle in the center of the room

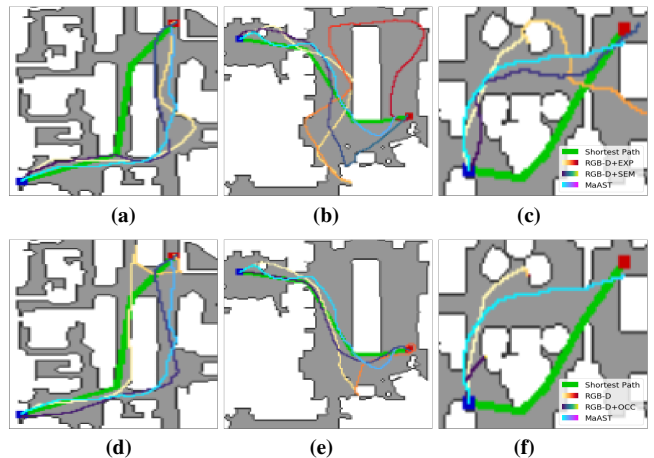


Fig. 4: A visualization of the path taken by different methods for three episodes from Matterport3D. The ground truth shortest path is shown by a solid green line. The agents’ start and goal locations are marked with a blue and red dot, respectively. The color of the agents’ paths shifts along a gradient (reproduced in the legend) as the maximum number of steps for the episode (500) is approached.

in Figure 4b) to move more efficiently towards the goal.

The final episode (Figures 4c and 4f) represents a failure case for all the methods. MaAST and RGBD+SEM reach close to the goal; however the episodes are registered as failures, as neither are within the 0.2 m success radius. On the other hand, RGBD+EXP completely misses the goal, heading off the visualized map into the next room, while both RGB-D and RGBD+OCC get stuck on the furniture and terminate. In our analysis, we find that for this particular Matterport3D house model, there appears to be holes in the 3D model towards the policy network; *e.g.*, all of the furniture at the bottom is fused together. However, one of the strengths of leveraging semantics in our models seems to be avoiding areas that either present narrow spaces with high collision potential or low-lying objects below the agent’s field of view. This is an instance when we observe the agent utilizing semantics of the environment (*i.e.*, “furniture is difficult to navigate through”) beyond just which areas are free and which are not.

V. CONCLUSION

In this paper, we introduced principled techniques for improved performance on visual navigation tasks with autonomous agents, by leveraging rich semantic features while simultaneously operating under a computational budget. Our proposed MaAST, incorporates a novel attention mechanism based on multi-layer Transformers, which encourages agents to focus on the most relevant areas of the egocentric semantic map for navigation. Through systematic experimentation with quantitative and qualitative analysis, we demonstrate the superior performance of our proposed approach as compared with several baselines. We show that MaAST provides significant performance gains (a 13% gain in path efficiency over purely visual methods), while also outperforming classical geometry-based methods with decreased training budget (time, computational requirements, and cost).

REFERENCES

- [1] N. Burgess, "Spatial cognition and the brain," *Annals of the New York Academy of Sciences*, vol. 1124, no. 1, pp. 77–97, 2008.
- [2] M. Denis and J. M. Loomis, "Perspectives on human spatial cognition: memory, navigation, and environmental learning," *Psychological Research*, vol. 71, no. 3, pp. 235–239, 2007.
- [3] S. Thrun, W. Burgard, and D. Fox, *Probabilistic robotics*. MIT press, 2005.
- [4] A. J. Davison and D. W. Murray, "Mobile robot localisation using active vision," in *ECCV*, 1998, pp. 809–825.
- [5] G. N. DeSouza and A. C. Kak, "Vision for mobile robot navigation: A survey," *IEEE transactions on pattern analysis and machine intelligence*, vol. 24, no. 2, pp. 237–267, 2002.
- [6] S. M. LaValle and J. J. Kuffner Jr, "Rapidly-exploring random trees: Progress and prospects," 2000.
- [7] J. Canny, *The complexity of robot motion planning*. MIT press, 1988.
- [8] L. E. Kavraki, P. Svestka, J.-C. Latombe, and M. H. Overmars, "Probabilistic roadmaps for path planning in high-dimensional configuration spaces," *IEEE transactions on Robotics and Automation*, vol. 12, no. 4, pp. 566–580, 1996.
- [9] M. Savva, A. Kadian, O. Maksymets, Y. Zhao, E. Wijmans, B. Jain, J. Straub, J. Liu, V. Koltun, J. Malik, D. Parikh, and D. Batra, "Habitat: A Platform for Embodied AI Research," in *ICCV*, 2019.
- [10] E. Wijmans, A. Kadian, A. Morcos, S. Lee, I. Essa, D. Parikh, M. Savva, and D. Batra, "Decentralized distributed ppo: Solving pointgoal navigation," *arXiv preprint arXiv:1911.00357*, 2019.
- [11] A. Vaswani, N. Shazeer, N. Parmar, J. Uszkoreit, L. Jones, A. N. Gomez, L. Kaiser, and I. Polosukhin, "Attention is all you need," in *NIPS*, 2017, pp. 5998–6008.
- [12] T. Chen, S. Gupta, and A. Gupta, "Learning exploration policies for navigation," in *ICLR*, 2019.
- [13] M. Jaderberg, V. Mnih, W. M. Czarnecki, T. Schaul, J. Z. Leibo, D. Silver, and K. Kavukcuoglu, "Reinforcement learning with unsupervised auxiliary tasks," *arXiv preprint arXiv:1611.05397*, 2016.
- [14] D. Pathak, P. Agrawal, A. A. Efros, and T. Darrell, "Curiosity-driven exploration by self-supervised prediction," in *CVPR workshops*, 2017, pp. 16–17.
- [15] S. Gupta, D. Fouhey, S. Levine, and J. Malik, "Unifying map and landmark based representations for visual navigation," *arXiv preprint arXiv:1712.08125*, 2017.
- [16] V. Mnih, A. P. Badia, M. Mirza, A. Graves, T. Lillicrap, T. Harley, D. Silver, and K. Kavukcuoglu, "Asynchronous methods for deep reinforcement learning," in *ICML*, 2016, pp. 1928–1937.
- [17] E. Kolve, R. Mottaghi, D. Gordon, Y. Zhu, A. Gupta, and A. Farhadi, "Ai2-thor: An interactive 3d environment for visual ai," *arXiv preprint arXiv:1712.05474*, 2017.
- [18] A. Dosovitskiy and V. Koltun, "Learning to act by predicting the future," *arXiv preprint arXiv:1611.01779*, 2016.
- [19] D. S. Chaplot, D. Gandhi, S. Gupta, A. Gupta, and R. Salakhutdinov, "Learning to explore using active neural SLAM," in *8th International Conference on Learning Representations, ICLR 2020, Addis Ababa, Ethiopia, April 26-30, 2020*. OpenReview.net, 2020. [Online]. Available: <https://openreview.net/forum?id=HklXn1BKDH>
- [20] M. Savva, A. X. Chang, A. Dosovitskiy, T. A. Funkhouser, and V. Koltun, "Minos: Multimodal indoor simulator for navigation in complex environments," *arXiv preprint arXiv:1712.03931*, 2017.
- [21] G. Brockman, V. Cheung, L. Pettersson, J. Schneider, J. Schulman, J. Tang, and W. Zaremba, "OpenAI gym," *arXiv preprint arXiv:1606.01540*, 2016.
- [22] F. Xia, A. R. Zamir, Z.-Y. He, A. Sax, J. Malik, and S. Savarese, "Gibson Env: Real-world perception for embodied agents," in *CVPR*, 2018, pp. 9068–9079.
- [23] M. Kempka, M. Wydmuch, G. Runc, J. Toczek, and W. Jaśkowski, "Vizdoom: A doom-based ai research platform for visual reinforcement learning," in *2016 IEEE Conference on Computational Intelligence and Games (CIG)*. IEEE, 2016, pp. 1–8.
- [24] C. Yan, D. Misra, A. Bennet, A. Walsman, Y. Bisk, and Y. Artzi, "Chalet: Cornell house agent learning environment," *arXiv preprint arXiv:1801.07357*, 2018.
- [25] S. Song, F. Yu, A. Zeng, A. X. Chang, M. Savva, and T. Funkhouser, "Semantic scene completion from a single depth image," in *CVPR*, 2017, pp. 1746–1754.
- [26] M. Fisher, D. Ritchie, M. Savva, T. Funkhouser, and P. Hanrahan, "Example-based synthesis of 3d object arrangements," *ACM Transactions on Graphics (TOG)*, vol. 31, no. 6, p. 135, 2012.
- [27] A. Handa, V. Patraucean, V. Badrinarayanan, S. Stent, and R. Cipolla, "Understanding real world indoor scenes with synthetic data," in *CVPR*, 2016, pp. 4077–4085.
- [28] A. X. Chang, A. Dai, T. A. Funkhouser, M. Halber, M. Nießner, M. Savva, S. Song, A. Zeng, and Y. Zhang, "Matterport3d: Learning from rgb-d data in indoor environments," *2017 International Conference on 3D Vision (3DV)*, pp. 667–676, 2017.
- [29] I. Armeni, O. Sener, A. R. Zamir, H. Jiang, I. Brilakis, M. Fischer, and S. Savarese, "3d semantic parsing of large-scale indoor spaces," in *CVPR*, 2016, pp. 1534–1543.
- [30] D. Mishkin, A. Dosovitskiy, and V. Koltun, "Benchmarking classic and learned navigation in complex 3d environments," *arXiv preprint arXiv:1901.10915*, 2019.
- [31] A. Sax, B. Emi, A. R. Zamir, L. J. Guibas, S. Savarese, and J. Malik, "Mid-level visual representations improve generalization and sample efficiency for learning active tasks," *arXiv preprint arXiv:1812.11971*, 2018.
- [32] W. B. Shen, D. Xu, Y. Zhu, L. J. Guibas, F. Li, and S. Savarese, "Situational fusion of visual representation for visual navigation," in *ICCV*, 2019.
- [33] B. Yamauchi, "A frontier-based approach for autonomous exploration," in *cira*, vol. 97, 1997, p. 146.
- [34] S. Thrun, M. Bennewitz, W. Burgard, A. B. Cremers, F. Dellaert, D. Fox, D. Hahnel, C. Rosenberg, N. Roy, J. Schulte, et al., "Minerva: A second-generation museum tour-guide robot," in *ICRA*, vol. 3. IEEE, 1999.
- [35] N. Savinov, A. Raichuk, R. Marinier, D. Vincent, M. Pollefeys, T. Lillicrap, and S. Gelly, "Episodic curiosity through reachability," *arXiv preprint arXiv:1810.02274*, 2018.
- [36] S. Gupta, J. Davidson, S. Levine, R. Sukthankar, and J. Malik, "Cognitive mapping and planning for visual navigation," in *CVPR*, 2017, pp. 7272–7281.
- [37] S. K. Ramakrishnan, Z. Al-Halah, and K. Grauman, "Occupancy anticipation for efficient exploration and navigation," in *Computer Vision - ECCV 2020 - 16th European Conference, Glasgow, UK, August 23-28, 2020, Proceedings, Part V*, ser. Lecture Notes in Computer Science, A. Vedaldi, H. Bischof, T. Brox, and J. Frahm, Eds., vol. 12350. Springer, 2020, pp. 400–418. [Online]. Available: https://doi.org/10.1007/978-3-030-58558-7_24
- [38] D. S. Chaplot, D. Gandhi, A. Gupta, and R. Salakhutdinov, "Object goal navigation using goal-oriented semantic exploration," *CoRR*, vol. abs/2007.00643, 2020. [Online]. Available: <https://arxiv.org/abs/2007.00643>
- [39] W. Yang, X. Wang, A. Farhadi, A. Gupta, and R. Mottaghi, "Visual semantic navigation using scene priors," *arXiv preprint arXiv:1810.06543*, 2018.
- [40] E. Parisotto and R. Salakhutdinov, "Neural map: Structured memory for deep reinforcement learning," *arXiv preprint arXiv:1702.08360*, 2017.
- [41] J. Oh, V. Chockalingam, S. P. Singh, and H. Lee, "Control of memory, active perception, and action in minecraft," *arXiv preprint arXiv:1605.09128*, 2016.
- [42] P. Anderson, A. X. Chang, D. S. Chaplot, A. Dosovitskiy, S. Gupta, V. Koltun, J. Kosecka, J. Malik, R. Mottaghi, M. Savva, and A. R. Zamir, "On evaluation of embodied navigation agents," *arXiv preprint arXiv:1807.06757*, 2018.
- [43] A. Mikhailov, "Turbo, an improved rainbow colormap for visualization," <https://ai.googleblog.com/2019/08/turbo-improved-rainbow-colormap-for.html>, 2019.
- [44] K. He, X. Zhang, S. Ren, and J. Sun, "Deep residual learning for image recognition," in *CVPR*, 2016, pp. 770–778.
- [45] J. Devlin, M.-W. Chang, K. Lee, and K. Toutanova, "Bert: Pre-training of deep bidirectional transformers for language understanding," in *NAACL-HLT*, 2019.
- [46] H. Zhang, I. J. Goodfellow, D. N. Metaxas, and A. Odena, "Self-attention generative adversarial networks," in *ICML*, ser. Proceedings of Machine Learning Research, vol. 97. PMLR, 2019, pp. 7354–7363.
- [47] L. H. Li, M. Yatskar, D. Yin, C. Hsieh, and K. Chang, "Visualbert: A simple and performant baseline for vision and language," *arXiv preprint arXiv:1908.03557*, 2019.
- [48] J. Lu, D. Batra, D. Parikh, and S. Lee, "Vilbert: Pretraining task-agnostic visiolinguistic representations for vision-and-language tasks," *arXiv preprint arXiv:1908.02265*, 2019.
- [49] K. Cho, B. van Merriënboer, Ç. Gülçehre, D. Bahdanau, F. Bougares, H. Schwenk, and Y. Bengio, "Learning phrase representations using

- RNN encoder-decoder for statistical machine translation,” in *EMNLP*, 2014, pp. 1724–1734.
- [50] J. Schulman, F. Wolski, P. Dhariwal, A. Radford, and O. Klimov, “Proximal policy optimization algorithms,” *arXiv preprint arXiv:1707.06347*, 2017.
- [51] A. Paszke, S. Gross, S. Chintala, G. Chanan, E. Yang, Z. DeVito, Z. Lin, A. Desmaison, L. Antiga, and A. Lerer, “Automatic differentiation in PyTorch,” in *NIPS Autodiff Workshop*, 2017.
- [52] T. Wolf, L. Debut, V. Sanh, J. Chaumond, C. Delangue, A. Moi, P. Cistac, T. Rault, R. Louf, M. Funtowicz, and J. Brew, “Huggingface’s transformers: State-of-the-art natural language processing,” *ArXiv*, vol. abs/1910.03771, 2019.
- [53] V. Cartillier, Z. Ren, N. Jain, S. Lee, I. Essa, and D. Batra, “Semantic mapnet: Building allocentric semanticmaps and representations from egocentric views,” *CoRR*, vol. abs/2010.01191, 2020. [Online]. Available: <https://arxiv.org/abs/2010.01191>